Non-homogeneous hidden Markov-switching models for wind time series

Pierre Ailliot, Julie Bessac, Valérie Monbet, Françoise Pene

Non-homogeneous hidden Markov-switching models for wind time series

Pierre Ailliot[1], Julie Bessac[2], Valérie Monbet [2], Françoise Pène [1]

April 7, 2014

[1] *Laboratoire de Mathématiques de Bretagne Atlantique, UMR 6205, Université de Brest, France*
[2] *Institut de Recherche Mathématiques de Rennes, UMR 6625, Université de Rennes 1, France*

Abstract

In this paper we propose various Markov-switching auotoregressive models for bivariate time series which describe wind conditions at a single location. The main originality of the proposed models is that the hidden Markov chain is not homogeneous, its evolution depending on the past wind conditions. It is shown that they permit to reproduce complex features of wind time series such as non-linear dynamics and the multimodal marginal distributions.

Keywords: Wind time series, Markov-switching autoregressive process, non-homogeneous hidden Markov process, linear-circular time series

1 Introduction

Wind time series are more and more involved in risk forecasting and impact studies applications. Wind data are often available over periods of time that are not long enough to estimate reliably probabilities of complex events related, for example, to the maintenance of wind farms (see [16]). Stochastic weather generators have been developed to overcome this insufficiency by simulating unlimited number of sequences as long as desired of meteorological variables with statistical properties similar to those of the observations.

In this paper, we have used the ERA-40 data set which consists in a global reanalysis with 6-hourly data covering the period from 1958 to 2001. This reanalysis was carried out by the European Centre for Medium-range Weather Forecast (ECMWF) and can be freely downloaded and used for scientific purposes at the URL: *http://data.ecmwf.int/data*. We have extracted from the ERA-40 data set the wind data for the point with geographical coordinates (47.5^0 N, 5^0 W) which is located off the Brittany coast (northwest of France). We have performed a comparison with in-situ data which indicates that this reanalysis data provides an accurate description of the wind condition observed at this location with the advantage of being easy to use in a statistical study (long time series with no missing data). The resulting time series is non-stationary since it exhibits an important seasonal component but also diurnal and inter-annual

components. A classical approach for treating seasonality in meteorological time series consists in blocking the data, typically by period ranging from a month to a trimester depending on the amount of data available, and fit a separate model for each period in the year. This approach has been used in this paper and we have chosen to focus on the months of January. It leads to 44 time series of length 124 (31 days with 4 observations each day), each time series describing the wind conditions during the months of January for a particular year. In the sequel, we assume that these time series are independent realizations of a stationary process. It seems realistic according to the results given in [2] for the wind speed at the same location since the diurnal components can be neglected during the winter season. Following [2], another approach would consist in letting some of the coefficients of the model introduced below to evolve in time with periodic functions for the diurnal and seasonal components and eventually a trend. The wind condition at a single location at time t can be described using the polar coordinates $\{U_t, \Phi_t\}$, where U_t denotes the wind speed with values in $\mathbb{R}^+$ and Φ_t the wind direction with values in $\mathbb{T} = \mathbb{R}/2\pi\mathbb{Z}$ or the Cartesian coordinates $\{u_t, v_t\}$ where u_t and v_t denote respectively the zonal and meridional components with values in $\mathbb{R}$.

The bivariate marginal distribution of the wind time series considered in this work has complex features (see Figure 1). In particular it clearly exhibits two modes, each one corresponding to a different meteorological regime or 'weather types': the prevailing mode corresponds to westerlies cyclonic conditions with low pressure systems coming from the Atlantic ocean whereas the second mode is associated to anticyclonic conditions and wind blowing from the east. The presence of regimes with distinct weather conditions is a usual feature of meteorological time series and a classical approach for modeling these meteorological regimes (or "weather types") consists in introducing a hidden (or latent) variable. This idea goes back to [22] where Hidden Markov Models (HMMs) were proposed for modeling the space-time evolution of daily rainfall (see [4] for more recent references on this topic). HMMs have also been proposed for modeling time series of wind direction in [23]. However HMMs assume that the successive observations are conditionally independent given the latent weather type and we found fail in reproducing the strong relation which exists between the wind conditions at successive time steps (see the time series on Figure 2). In this situation it seems natural to consider Markov-Switching AutoRegressive (MS-AR) models which extend the usual HMMs by adding dynamics in the regimes (Section 2). MS-AR models are also an extension of AR models which are often used to model wind time series.

In HMMs or MS-AR models, the evolution of the weather type is independent of the past observed process. For our particular example, it would imply for example that the probability of switching from the cyclonic conditions to the anticyclonic conditions between time t and time $t+1$ does not dependent on the wind conditions observed at time t whereas we know that these switchings generally occur when the wind is blowing from the North and is very unlikely to occur when the wind is blowing from the South. The main originality of the models proposed in this paper is that the evolution of the latent weather type depends on past wind direction leading to non-homogeneous MS-AR (NHMS-AR) models. We show that NHMS-AR models lead to a better description of important characteristics of the data considered in this work, such as multimodality and non-linear dynamics, compared to MS-AR models.

The polar coordinates are generally used by meteorologists, probably because they are easier to interpret. However, from a statistical point of view, it is probably easier to model the time series of Cartesian components $\{u_t, v_t\}$ since many models have been proposed for bivariate time series with values in $\mathbb{R}^2$. The process $\{U_t, \Phi_t\}$ is a linear-circular process with values in $\mathbb{R}^+ \times \mathbb{T}$ and few models have been proposed for such variables. Both representations have their advantages and it is not easy to decide a priori which one to choose.

The paper is organized as follows. NHMS-AR models are introduced in Section 2 with specific parameterizations proposed when considering Cartesian and polar coordinates. Parameter estimation is discussed in Section 3. Then the performances of the models are discussed and compared in Section 4. At last, we make a synthesis of the obtained results and we give some perspectives in Section 5.

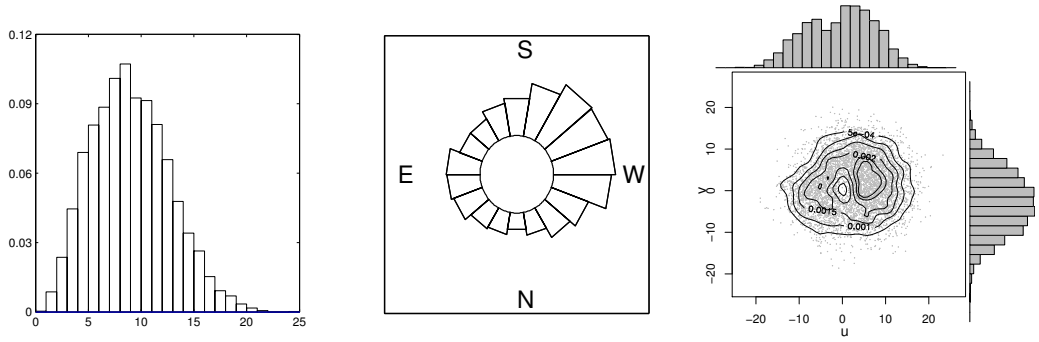

Figure 1: Histogram of $\{U_t\}$ (left), rose plot of $\{\Phi_t\}$ (middle) and histograms of $\{u_t\}$ and $\{v_t\}$ and joint distribution of $\{u_t, v_t\}$ (right). The lines on the scatter plots are levels of a non-parametric kernel estimate of the bivariate density. Results for the months of January.

2 Models

2.1 Non-homogeneous Markov-switching autoregressive models

Let $X_t \in \{1, ..., M\}$ represent the latent weather type and Y_t denote the observed wind conditions at time t. Throughout the article $\{Y_t\}$ will represent successively the bivariate process of Cartesian coordinates of wind in Section 2.3, the wind direction in Section 2.4, and finally $\{Y_t\}$ stands for the wind speed in Section 2.5. Let us write $\mathbb{E}$ the space in which Y_t takes values, $\mathbb{E}$ will respectively refer to $\mathbb{R}^2$, $\mathbb{T}$ and $\mathbb{R}^+$. It will be useful to introduce notation $Y_t^{t+u} := (Y_t, ..., Y_{t+u})$, $y_t^{t+u} := (y_t, ..., y_{t+u})$ (as well as X_t^{t+u}, x_t^{t+u}) for $t > 0$ and $u > 0$.

Hypothesis 1. *Let $s, M \geq 1$ be some integers. The sequence $(X_t, Y_{t-s+1}^t)_{t\in\mathbb{Z}}$ follows a NHMS-AR model if it is a Markov chain with values in $\{1, ..., M\} \times \mathbb{E}$ such that*

- *the conditional distribution of X_t given the values of $\{X_{t'}\}_{t'<t}$ and $\{Y_{t'}\}_{t'<t}$ only depends on X_{t-1} and Y_{t-1} and we denote $p_1(x_t|x_{t-1}, y_{t-1}) = P(X_t = x_t|X_{t-1} = x_{t-1}, Y_{t-1} = y_{t-1})$,*
- *the conditional distribution of Y_t given the values of $\{Y_{t'}\}_{t'<t}$ and $\{X_{t'}\}_{t'\leq t}$ only depends on X_t and $Y_{t-1}, \ldots, Y_{t-s}$ and this conditional distribution has a probability density function (p.d.f.) $p_2\left(y_t|x_t, y_{t-s}^{t-1}\right)$.*

Let us write $p(.|x_{t-u}^{t-1}, y_{t-u}^{t-1})$ for the conditional p.d.f. of (X_t, Y_t) given $(X_{t-u}^{t-1} = x_{t-u}^{t-1}, Y_{t-u}^{t-1} = y_{t-u}^{t-1})$. Hypothesis 1 implies that for $u \geq s$

$$p(x_t, y_t|x_{t-u}^{t-1}, y_{t-u}^{t-1}) = p_1(x|x_{t-1}, y_{t-1})p_2(y|x, y_{t-s}^{t-1}). \tag{1}$$

The various conditional independence assumptions are summarized by the directed graph below for $s = 1$. They define a quite general family of model which will be referred to as Non-Homogeneous Markov-Switching AutoRegressive (NHMS-AR) models in the sequel.

$$\begin{array}{ccccccccc} \cdots & \to & X_{t-1} & \to & X_t & \to & X_{t+1} & \to & \cdots \\ & & \downarrow & \nearrow & \downarrow & \nearrow & \downarrow & & \\ \cdots & \to & Y_{t-1} & \to & Y_t & \to & Y_{t+1} & \to & \cdots \end{array}$$

NHMS-AR models define a quite general family of models:

- If $p_1(x_t|x_{t-1}, y_{t-1})$ does not depend on y_{t-1}, we retrieve the usual MS-AR models which include the HMMs as a particular case ($s = 0$).
- If $M = 1$, $\{Y_t\}$ is an autoregressive process of order s.
- If $p_{1,\theta}(x_k|x_{k-1}, y_{k-s}^{k-1})$ does not dependent on x_{k-1} and is parametrized using indicator functions, we obtain the Threshold AutoRegressive (TAR) models which is an other important family of models with regime switching in the literature (see e.g. [20]).

The following sections propose specific parametric models for p_1 (see Section 2.2) and p_2 when using Cartesian coordinates (see 2.3) or polar coordinates (see Sections 2.4 and 2.5).

2.2 Modeling weather types

As mentioned earlier, we introduce the latent process $\{X_t\}$ to describe the weather type which evolution may depend on previous wind direction. For example, we expect that the probability of switching from the cyclonic to the anticyclonic conditions generally is more likely to occur when the wind is blowing from the North that when it is blowing from the South. Such feature can be modeled through the transition kernel p_1. In all the models we assume more precisely that

$$p_1(x_t|x_{t-1}, \phi_{t-1}) \propto q_{x_{t-1},x_t} f_{VM}(\phi_{t-1}; \kappa = \lambda_{x_{t-1},x_t}, \phi = \psi_{x_{t-1},x_t}), \tag{2}$$

where $f_{VM}(.; \kappa, \phi)$ is the probability density function (p.d.f) of the von Mises distribution, $Q = (q_{x,x'})_{x,x' \in \{1,...,M\}}$ is a stochastic matrix with positive entries and, for $x, x' \in \{1, ..., M\}$, $\lambda_{x,x'} \geq 0$ and $\psi_{x,x'} \in \mathbb{T}$ are unknown parameters. The von Mises distribution is a natural distribution for circular variables (see [19]) which p.d.f. with respect to the Lebesgue measure on $\mathbb{T}$, is given by

$$\forall z \in \mathbb{T}, \quad f_\gamma(z) := f_{VM}(z; \kappa, \phi) = \frac{1}{2\pi I_0(\kappa)} \exp\left(\kappa \cos(z - \phi)\right) = \frac{1}{2\pi I_0(|\gamma|)} \left| e^{\gamma e^{-iz}} \right|, \tag{3}$$

for $\Phi \in \mathbb{T}$ and $\gamma := \kappa e^{i\phi}$ is a complex parameter. I_0 denotes the modified Bessel function of order 0 defined as

$$I_0(\kappa) := \frac{1}{2\pi} \int_{\mathbb{T}} \exp(\kappa \cos(z))\, dz.$$

$\phi \in \mathbb{T}$ corresponds to the circular mean of the distribution and $\kappa \geq 0$ describes the concentration of the distribution around ϕ: when $\kappa = 0$ we get the uniform distribution whereas when κ increases the distribution is more and more concentrated around ϕ. This distribution is denoted by $VM(\gamma)$ hereafter.

According to (2), the probability that the hidden Markov chain $\{X_t\}$ switches from x_{t-1} to x_t will increase when the wind direction Φ_{t-1} is close to ψ_{x_{t-1},x_t} and λ_{x_{t-1},x_t} models the directional spreading in which this transition is likely to occur. When $\lambda_{x,x'} = 0$ for all $x, x' \in \{1, ..., M\}$ then we obtain again the homogeneous MS-AR models. Observe that (2) can be rewritten

$$p_1(x_t|x_{t-1}, \phi_{t-1}) = \frac{q_{x_{t-1},x_t} \left|\exp\left(\tilde{\lambda}_{x_{t-1},x_t} e^{-i\phi_{t-1}}\right)\right|}{\sum_{x'=1}^{M} q_{x_{t-1},x'} \left|\exp\left(\tilde{\lambda}_{x_{t-1},x'} e^{-i\phi_{t-1}}\right)\right|}, \tag{4}$$

with $\tilde{\lambda}_{x,x'} \in \mathbb{C}$ (by taking $\tilde{\lambda}_{x,x'} = \lambda_{x,x'} e^{i\psi_{x,x'}}$). With this expression, it can be easily seen that replacing $(\tilde{\lambda}_{x,x'})_{x,x'}$ by $(\tilde{\lambda}_{x,x'} - a_x)_{x,x'}$ (for any choice of $(a_x)_x$) does not change p_1 and thus that identifiability constraints are needed.

In order to reduce the number of unknown parameters we add the following constraints for the non-homogeneous models developed in the sequel

$$\tilde{\lambda}_{x,x'} = \tilde{\lambda}_{x'} \tag{5}$$

for all $x, x' \in \{1, ..., M\}$ such that $x \neq x'$ with the identifiability constraint

$$\sum_{x'=1}^{M} \tilde{\lambda}_{x'} = 0 \tag{6}$$

We have also fitted the model without the constraint (5) and found that the likelihood of these models is similar to the one of the models with the constraint (5) whereas they have a significantly larger number of parameters. Even when assuming (5), we found that the parameter $(\lambda_{x'})$ is sometimes hard to fit in practice and that fixing its values to e.g. the concentration parameter of the von-Mises distribution fitted to the time series of wind direction leads to satisfactory models. The results obtained with these alternative strategies are not further discussed below.

2.3 Modeling $\{u_t, v_t\}$ conditionally to the weather type

In this section we propose a model for the bivariate process $\{Y_t\} = \{u_t, v_t\}$ conditionally to the weather type $\{X_t\}$. This process has values in $\mathbb{R}^2$ and the most classical autoregressive model for such process is the linear Gaussian vector autoregressive (VAR) model of order s. With this model, if $X_t = x_t$ then

$$Y_t = A_0^{(x_t)} + A_1^{(x_t)} Y_{t-1} + ... + A_s^{(x_t)} Y_{t-s} + \left(\Sigma^{(x_t)}\right)^{\frac{1}{2}} \epsilon_t \tag{7}$$

where $A_l^{(x)} \in \mathbb{R}^2$ for $l \in \{0, ..., s\}$ and $x \in \{1, ..., M\}$, $\Sigma^{(x)} \in \mathbb{R}^2$ are symmetric positive matrices for $x \in \{1, ..., M\}$ and $\{\epsilon_t\}$ is a bivariate white noise sequence.

VAR models have been proposed for wind fields in a space-time context in [15, 3, 21, 12]. On our particular dataset, we found that it was not appropriate to reproduce the 'hole' around the origin which can be seen on the joint distribution on Figure 1. It corresponds to a low probability of observing low wind speed. We can get around this issue by applying a power transformation as follows

$$\left\{ \begin{array}{rcl} \tilde{u}_t & = & U_t^{\alpha} \cos(\Phi_t) \\ \tilde{v}_t & = & U_t^{\alpha} \sin(\Phi_t) \end{array} \right.$$

and fit the MS-AR model is fitted the Gaussian model to $\{\tilde{u}_t, \tilde{v}_t\}$ instead of $\{u_t, v_t\}$. The value $\alpha = 1.5$ was chosen experimentally to remove the 'hole' close to the origin in the original distribution. The model with homogeneous hidden Markov chain is denoted **HMS-AR**$_{(u,v)}$ and the non-homogeneous model, where p_1 is given by (2), is denoted **NHMS-AR**$_{(u,v)}$.

2.4 Modeling the wind direction conditionally to the weather type

In this section we propose a model for the circular process $\{Y_t\} = \{\Phi_t\}$. The inclusion of $\{U_t\}$ in this model is discussed in the next section. Several models have been proposed in the literature for circular time series The model proposed in this paper extends the models proposed in [6] and [13].

Several autoregressive models have been proposed in the literature for modeling directional time series (see [6], [10],[13], [18]). We have chosen to focus on the von Mises process initially introduced in [6] and assume that the conditional distribution of Y_t given $\left(X_t = x_t, Y_{t-s}^{t-1} y_{t-s}^{t-1}\right)$ is $VM\left(\gamma_0^{(x_t)} + \sum_{\ell=1}^{s} \gamma_\ell^{(x_t)} e^{iy_{t-\ell}}\right)$ with $\gamma_\ell^{(x)} = \kappa_\ell^{(x)} e^{i\phi_\ell^{(x)}} \in \mathbb{C}$ for $x \in \{1, ..., M\}$ and $\ell \in \{0, ..., s\}$. This can be rewritten

$$\begin{aligned} p_2(y_t|x_t, y_{t-s}^{t-1}) &= \frac{1}{b(x_t, y_{t-s}^{t-1})} \exp\left(\kappa_0^{(x_t)} \cos(y_t - \phi_0^{(x_t)}) + \sum_{\ell=1}^{s} \kappa_\ell^{(x_t)} \cos(y_t - y_{t-\ell} - \phi_\ell^{(x)})\right) \\ &= \frac{1}{b(x_t, y_{t-s}^{t-1})} \left|\exp\left([\gamma_0^{(x_t)} + \sum_{\ell=1}^{s} \gamma_\ell^{(x_t)} e^{iy_{t-\ell}}] e^{-iy_t}\right)\right| \end{aligned} \tag{8}$$

with

$$\begin{aligned} b(x_t, y_{t-s}^{t-1}) &:= \int_{\mathbb{T}} \exp\left(\kappa_0^{(x_t)} \cos(y - \phi_0^{(x_t)}) + \sum_{\ell=1}^{s} \kappa_\ell^{(x_t)} \cos(y - y_{t-\ell})\right) dy \\ &= I_0\left(\left|\gamma_0^{(x_t)} + \sum_{\ell=1}^{s} \gamma_\ell^{(x_t)} e^{iy_{t-\ell}}\right|\right). \end{aligned}$$

In [6], it was assumed that $\gamma_\ell^{(x)} \in \mathbb{R}$ for $\ell \in \{1, ..., s\}$. We have chosen to extend it to a model with complex parameters in order to be able to reproduce the prevailing rotation of the wind direction in the clockwise direction (see Section 4).

The model with homogeneous hidden Markov chain is denoted **HMS-EVM** and the non-homogeneous model, where p_1 is given by (2), is denoted **NHMS-EVM**.

2.5 A joint model for the wind speed and wind direction

In [2] it was proposed to model the wind speed $\{U_t\}$ using a homogeneous MS-AR model with $M = 3$ regimes and Gaussian linear AR models (see (7)) of order $s = 2$. Figure 2 shows typical examples of wind speed and wind direction time series together with the regimes identified by the fitted MS-AR models. They basically correspond to periods with different temporal variability and there seems to be no simple relation between the regimes identified on the two time series. In this context, it does not seem relevant to use the same weather type for the two time series.

We thus propose to introduce a different weather type $X_t^{(U)}$ for the wind speed and $X_t^{(\Phi)}$ for the wind direction.

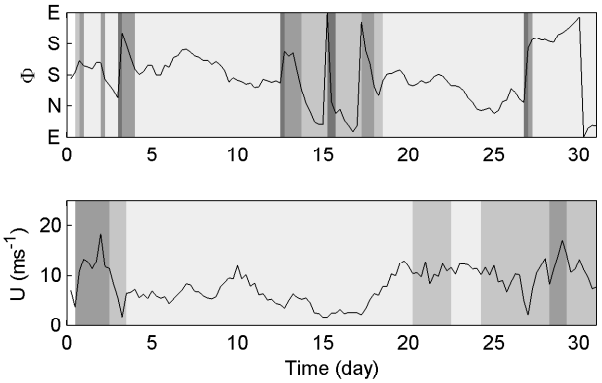

Figure 2: Example of time series of wind direction (top plot) and wind speed (bottom plot). The colors indicate the most likely regimes for the fitted **NHMS-EVM** model with 4 regimes (top plot) and Gaussian homogeneous MS-AR model for wind speed with 3 regimes (bottom plot). The regimes have been ordered according to the time variability (the darker the more variability).

In order to explore the link between $X_t^{(U)}$ and Φ, we have computed the most likely values of $X_t^{(U)}$ given the observed time series of wind speed $\{U_t\}$ and produced rose plots of the wind direction in the different weather types which were identified for the wind speed. We got plots very similar to the ones shown on Figure 3 (right panel). The first regime, which corresponds to periods with low temporal variability for the wind speed, can occur in any wind direction whereas the more variable regimes 2 and 3 are mainly associated to south-westerlies (cyclonic conditions).

It suggests the use of a non-homogeneous MS-AR model for the wind speed where the transition probabilities depend on the wind direction. Herefater $\mathbf{NHMS\text{-}AR}_{(U,\Phi)}$ denote the model for $\{U_t, \Phi_t\}$ such that

- $\{\Phi_t\}$ is modeled by the **NHMS-EVM** model for $\{x_t^{(\Phi)}, \Phi_t\}$ with $M = 4$ and $s = 2$,
- $\{U_t\}$ is modeled conditionally to $\{\Phi_t\}$ by a NHMS-AR model with p_1 given by (2) and p_2 by a linear Gaussian AR model (7).

The structure of the model, with two layers of hidden variables, one for the wind speed and one for the wind direction, is shown on the directed graph below.

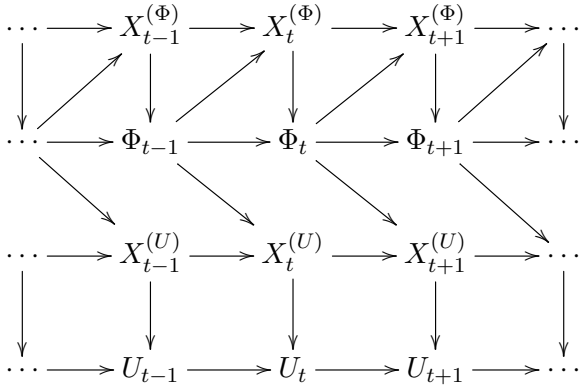

3 Parameter estimation

3.1 Numerical computation of the maximum likelihood estimate

The parameter vector of NH-MSAR models is composed of the parameters θ_Q of the transition probabilities $p_1(x_t|x_{t-1}, y_{t-1})$, the parameters $\theta^{(x)}$ of the transition kernel $p_2(y_t|x, y_{t-s}^{t-1})$ for each regime $x \in \{1, ..., M\}$ and the initial distribution of the regimes.

They are estimated by maximizing the likelihood function using a generalized EM algorithm. This algorithm was initially introduced in [5] for HMMs and then generalized to models with latent variables in [8]. This recursive algorithm computes successive approximations $\hat{\theta}_i$ of the maximum likelihood estimate (MLE). $\hat{\theta}$ by cycling through the following steps.

E-step: Compute $Q\left(\theta|\hat{\theta}_i\right) = E_{\hat{\theta}_i}(\log(p_\theta(X_1^T, Y_1^T))|y_{-s+1}^T)$ as a function of θ.

M-step: Determine the updated parameter estimate $\hat{\theta}_{i+1} = \arg\max_\theta Q\left(\theta|\hat{\theta}_i\right)$.

The conditional probabilities involved in the computation of $Q(\theta|\hat{\theta}_n)$ are computed using the so-called forward-backward recursions (see e.g. [7] and references therein). The particular implementation of these recursions for homogeneous MS-AR models is discussed in [14] and [17] discusses it for non-homogeneous HMMs. It can be easily generalized to the models considered in this paper. The M-step requires numerical optimization leading to the so-called Generalized EM (GEM) algorithm. In order to get an efficient EM algorithm, it is important to implement carefully the numerical optimization procedure. In practice, the function $Q(.|\hat{\theta}_i)$ which has to be maximized in the M-step can be written as the sum of $M + 1$ functions as follows

$$Q\left(\theta|\hat{\theta}_i\right) = Q_X\left(Q, \theta_Q|\hat{\theta}_i\right) + \sum_{x=1}^{M} Q_Y\left(\theta^{(x)}|\hat{\theta}_i\right).$$

This leads to solving $M + 1$ separate optimization problems on spaces with reduced dimension which is far more efficient than maximizing directly $Q(.|\hat{\theta}_i)$ over all the parameters. Note that analytical expressions are available for the Gaussian linear AR models (7).

In order to avoid convergence to non-interesting maxima and save computational time, a proper initialization of this algorithm with realistic parameter values $\hat{\theta}_0$ is needed. In practice, we have used the nested nature of the models. We have first fitted homogeneous models and then use the estimated parameters as a starting point for the corresponding non-homogeneous models. In the same spirit, the results obtained for the model of order s have been used to initialize the EM for the models of order $s + 1$.

3.2 Properties

All the models considered here are ψ-irreducible, Harris-recurrent. Moreover, for these models, the parameters are identifiable up to a permutation of indices and the Maximum Likelihood Estimator is consistent.

In this section we prove ψ-irreducibility, aperiodicity, Harris-recurrence, identifiability and consistency for the NHMS-EVM. One can prove the same results for the other models by combining arguments of this appendix with those of [1, section 2.2]

Assume Hypothesis 1 with p_1 and p_2 given by (4) and (8) respectively.

Let Θ' be the set of parameters $\theta = (q_{x,x'}, \tilde{\lambda}_{x,x'}, \gamma_\ell^{(x)})_{\ell,x,x'}$ such that $\gamma_\ell^{(x)} \in \mathbb{C}$, $q_{x,x'} > 0$ such that $\sum_{x'} q_{x,x'} = 1$ and $\tilde{\lambda}_{x,x'} \in \mathbb{C}$ satisfying (6).

Theorem 2 (Consistency for NHMS-EVM)**.** *Assume that Θ is a compact subset of Θ' and that the coordinates of the true parameter θ^* satisfy*

$$x \neq x' \;\Rightarrow\; (\gamma_{0,*}^{(x)}, ..., \gamma_{s,*}^{(x)}) \neq (\gamma_{0,*}^{(x')}, ..., \gamma_{s,*}^{(x')}). \tag{9}$$

Then, for every $x_0 \in \{1, ..., M\}$ and any initial measure ν on $\{1, ..., M\} \times \mathbb{T}$, on a set of probability one, the limit values $\theta = (\gamma, Q, \tilde{\lambda})$ of the sequence of MLE $(\hat{\theta}_{n,x_0})_n$ are equal to $\theta^* = (\gamma_*, Q_*, \tilde{\lambda}_*)$ up to a permutation of indices, i.e. for any such limit value θ, there exists a permutation σ of $\{1, ..., M\}$ such that, for every $x, x' \in \{1, ..., M\}$, for every $j = 0, ..., s$, the following relations hold true

$$\gamma_j^{(x)} = \gamma_{j,*}^{(\sigma(x))}, \quad q_{x,x'} = q_{\sigma(x),\sigma(x'),*} \quad \textit{and} \quad \tilde{\lambda}_{x,x'} = \tilde{\lambda}_{\sigma(x),\sigma(x'),*}.$$

One can notice that (9) just means that there is no couple of regimes (x, x') with $x \neq x'$ in which the behaviour of the process Y is the same.

The proof of Theorem 2 is based on two ingredients: a general consistency result established in [1][Thm 2] and the proof of the "identifiability up to a permutation of indices".

Since for every $(\theta, x, y) \in \tilde{\Theta} \times \{1, ..., M\} \times \mathbb{T}$, $q_\theta(x, y|\cdot, \cdot)$ is continuous on the compact set $\{1, ..., M\} \times \mathbb{T}^s$, we have

$$\alpha = \int_{E \times K} \gamma(x, y)\, d\mu_0(x, y) > 0, \quad \text{with} \quad \gamma(x, y) := \inf_{x', y_{-s}^{-1}} q_\theta(x, y|x', y_{-s}^{-1}).$$

Now we consider the probability density function (w.r.t. μ_0) β given by

$$\beta(x, y) := \frac{\gamma(x, y)}{\alpha}.$$

For every $x_0, x_{-1} \in E$ and every y_{-s}^0, we have

$$q_\theta(x_0, y_0|x_{-1}, y_{-s}^{-1}) \geq \alpha\beta(x_0, y_0).$$

This implies the ψ-irreducibility, strongly aperiodic (the ν_1-small set being the whole space), the Harris recurrence (since we can decompose the whole set in a union of uniformly accessible sets from the whole set), positive (the invariant measure being unique and finite). In particular, this gives Assumption (5) of [1][Thm 2].

Moreover, since $p_{1,\theta}(x_1|x_0, y_0)$ and $p_{2,\theta}(y_0|x_0, y_{-1})$ are continuous in (θ, x_1, x_0, y_0) and in $(\theta, x_0, y_0, y_{-1})$ (respectively), all the other assumptions of [1][Thm 2] are satisfied for any compact subset of Θ'. Hence, we have

Corollary 3. *Assume that Θ is a compact subset of Θ'. Then, for all $\theta \in \Theta$, there exists a unique invariant probability and, for every $x_0 \in E$ and every initial probability ν, the limit values of $(\hat{\theta}_{n,x_0})_n$ are $\bar{\mathbb{P}}_{\theta^*}$-almost surely contained in $\{\theta \in \Theta \;:\; \bar{\mathbb{P}}_\theta = \bar{\mathbb{P}}_{\theta^*}\}$.*

Now, Theorem 2 will follow from the following result giving the identifiability of the parameter (up to permutation of indices) .

Proposition 4 (Identifiability). *Let θ_1 and θ_2 belong to Θ' (resp. Θ''):*

$$\theta_i = \left((\gamma^{(x)}_{j,(i)})_{j,x}, (q_{x,x',(i)})_{x,x'}, (\tilde{\lambda}_{x,x',(i)})_{x,x'} \right).$$

Assume that the parameters $(\gamma^{(x)}_{j,(1)})_{j,x}$ which model the evolution of the wind direction in the different regimes through (8) for θ_1 are such that

$$x \neq x' \;\Rightarrow\; (\gamma^{(x)}_{0,(1)}, ..., \gamma^{(x)}_{s,(1)}) \neq (\gamma^{(x')}_{0,(1)}, ..., \gamma^{(x')}_{s,(1)}). \tag{10}$$

Then $\bar{\mathbb{P}}^Y_{\theta_1} = \bar{\mathbb{P}}^Y_{\theta_2}$ if and only θ_1 is equal to θ_2 up to a permutation of indices.

Proof of Proposition 4. We write Leb for the Lebesgue measure on $\mathbb{T}$. Assume that $\bar{\mathbb{P}}^Y_{\theta_1} = \bar{\mathbb{P}}^Y_{\theta_2}$. In particular, we have

$$\bar{p}_{\theta_1}(Y_t = y_t | Y^{t-1}_{t-s} = y^{t-1}_{t-s}) = \bar{p}_{\theta_2}(Y_t = y_t | Y^{t-1}_{t-s} = y^{t-1}_{t-s}), \text{ for } \bar{\mathbb{P}}^{Y^t_{t-s}}_{\theta_1} - a.e.\ y^t_{t-s}$$

and thus

$$\sum_{x=1}^M \bar{\mathbb{P}}_{\theta_1}(X_t = x | y^{t-1}_{t-s}) p_{2,\theta_1}(y_t | x, y^{t-1}_{t-s}) = \sum_{x=1}^M \bar{\mathbb{P}}_{\theta_2}(X_t = x | y^{t-1}_{t-s}) p_{2,\theta_2}(y_t | x, y^{t-1}_{t-s}), \text{ for } \bar{\mathbb{P}}^{Y^t_{t-s}}_{\theta_1} - a.e.\ y^t_{t-s}.$$

Since $\bar{p}_{\theta_1}(y^t_{t-s}) > 0$ (since the invariant density h_1 satisfies $h_1 > 0$ since $\alpha > 0$ and the transition density p satisfies $p > 0$ by construction) and since (4) holds true, we deduce that, for $\mathrm{Leb}^{\otimes(s+1)}$-a.e. y^t_{t-s}, we have

$$\sum_{x=1}^M \bar{\mathbb{P}}_{\theta_1}(X_t = x | y^{t-1}_{t-s}) f_{\gamma^{(x)}_{0,(1)} + \sum_{\ell=1}^s \gamma^{(x)}_{\ell,(1)} e^{iy_{t-\ell}}}(y_t) = \sum_{x=1}^M \bar{\mathbb{P}}_{\theta_2}(X_t = x | y^{t-1}_{t-s}) f_{\gamma^{(x)}_{0,(2)} + \sum_{\ell=1}^s \gamma^{(x)}_{\ell,(2)} e^{iy_{t-\ell}}}(y_t)$$

with f_γ defined by (3). Due to [11], finite mixtures of von Mises distributions are identifiable. Hence if

$$\sum_{x=1}^M \pi^{(x)}_1 f_{\gamma^{(x)}_1}(y) = \sum_{x=1}^M \pi^{(x)}_2 f_{\gamma^{(x)}_2}(y) \text{ for Leb} - a.e.\ y$$

with $\gamma^{(x)}_1 \neq \gamma^{(x')}_1$ for $x \neq x'$ and $\pi^{(x)}_1 > 0$ for $x \in \{1, ..., M\}$ then there exists a permutation $\tau : \{1, ..., M\} \to \{1, ..., M\}$ such that $\gamma^{(x)}_1 = \gamma^{(\tau(x))}_2$ and $\pi^{(x)}_1 = \pi^{(\tau(x))}_2$.

Recall that we have assumed that $\theta^{(x)}_{Y,1} \neq \theta^{(x')}_{Y,1}$ if $x \neq x'$, which implies that

$$for\ \mathrm{Leb}^{\otimes s} - a.e.\ y^{t-1}_{t-s}, \quad \gamma^{(x)}_{0,1} + \sum_{\ell=1}^s \gamma^{(x)}_{\ell,1} e^{iy_{t-\ell}} \neq \gamma^{(x')}_{0,1} + \sum_{\ell=1}^s \gamma^{(x')}_{\ell,1} e^{iy_{t-\ell}} \text{ for Leb} - a.e.\ y_t.$$

Therefore, since for every $x \in \{1, ..., M\}$ and for $\mathrm{Leb}^{\otimes s}$-almost every y^{t-1}_{t-s}, $\bar{\mathbb{P}}_{\theta_1}(X_t = x | y^{t-1}_{t-s}) > 0$ (since $h_{\theta_1} > 0$), for $\mathrm{Leb}^{\otimes s}$-almost every y^{t-1}_{t-s} there exists a permutation $\sigma_{y^{t-1}_{t-s}}$ of $\{1, ..., M\}$ such that,

$$\forall x \in \{1, ..., M\}, \quad \gamma^{(x)}_{0,(1)} + \sum_{\ell=1}^s \gamma^{(x)}_{\ell,(1)} e^{iy_{t-\ell}} = \gamma^{(\sigma_{y^{t-1}_{t-s}}(x))}_{0,(2)} + \sum_{\ell=1}^s \gamma^{(\sigma_{y^{t-1}_{t-s}}(x))}_{\ell,(2)} e^{iy_{t-\ell}}.$$

Since the set of permutations of $\{1, ..., M\}$ is finite, there exists a positive Lebesgue measure subset of $\mathbb{T}^s$ on which the permutation is the same permutation σ. From this, we deduce that

$$\forall x \in \{1, ..., M\},\ \forall j \in \{0, ..., s\}, \quad \gamma^{(x)}_{j,(1)} = \gamma^{(\sigma(x))}_{j,(2)}$$

and that, for Lebesgue almost every y_{t-s}^{t+1}, the following holds true

$$\forall x \in \{1,...,M\}, \bar{\mathbb{P}}_{\theta_1}(X_t = x|y_{t-s}^{t-1}) = \bar{\mathbb{P}}_{\theta_2}(X_t = \sigma(x)|y_{t-s}^{t-1}).$$

Let us now discuss the identifiability of the other components of θ_1 and θ_2. If $\bar{\mathbb{P}}_{\theta_1}^Y = \bar{\mathbb{P}}_{\theta_2}^Y$ then

$$\bar{p}_{\theta_1}(Y_t = y_t, Y_{t+1} = y_{t+1}|Y_{t-s}^{t-1} = y_{t-s}^{t-1}) = \bar{p}_{\theta_2}(Y_t = y_t, Y_{t+1} = y_{t+1}|Y_{t-s}^{t-1} = y_{t-s}^{t-1})\ \bar{\mathbb{P}}_{\theta_1}^Y\ a.s.$$

and thus, for Lebesgue almost every y_{t-s}^{t+1}, we have

$$\begin{aligned}
&\sum_{x,x'=1}^{M} \bar{\mathbb{P}}_{\theta_1}(X_t = x|y_{t-s}^{t-1}) p_{1,\theta_1}(x'|x, y_t) f_{\gamma_{0,(1)}^{(x)} + \sum_{\ell=1}^{s} \gamma_{\ell,(1)}^{(x)} e^{iy_{t-\ell}}}(y_t) f_{\gamma_{0,(1)}^{(x')} + \sum_{\ell=1}^{s} \gamma_{\ell,(1)}^{(x')} e^{iy_{t-\ell+1}}}(y_{t+1}) \\
= &\sum_{x,x'=1}^{M} \bar{\mathbb{P}}_{\theta_2}(X_t = x|y_{t-s}^{t-1}) p_{1,\theta_2}(x'|x, y_t) f_{\gamma_{0,(2)}^{(x)} + \sum_{\ell=1}^{s} \gamma_{\ell,(2)}^{(x)} e^{iy_{t-\ell}}}(y_t) f_{\gamma_{0,(2)}^{(x')} + \sum_{\ell=1}^{s} \gamma_{\ell,(2)}^{(x')} e^{iy_{t-\ell+1}}}(y_{t+1}).
\end{aligned}$$

This implies that, for almost every y_{t-s}^{t+1}, the quantity

$$\sum_{x,x'} \bar{\mathbb{P}}_{\theta_1}(X_t = x|y_{t-s}^{t-1})(p_{1,\theta_1}(x'|x, y_t) - p_{1,\theta_2}(\sigma(x')|\sigma(x), y_t)) f_{\gamma_{0,(1)}^{(x)} + \sum_{\ell=1}^{s} \gamma_{\ell,(1)}^{(x)} e^{iy_{t-\ell}}}(y_t) f_{\gamma_{0,(1)}^{(x')} + \sum_{\ell=1}^{s} \gamma_{\ell,(1)}^{(x')} e^{iy_{t-\ell+1}}}(y_{t+1})$$

is null and so (again using the identifiability of von Mises distribution)

$$\forall x, x',\quad p_{1,\theta_1}(x'|x, y_t) = p_{1,\theta_2}(\sigma(x')|\sigma(x), y_t) \text{ for Leb}-a.e.\ y_t.$$

Now, due to the special form of $p_{1,\theta}$ specified in (4), we get

$$\forall x, x',\ \text{Leb}-a.e.\ y_t,\ \frac{q_{x,x',(1)} \left|\exp\left(\tilde{\lambda}_{x,x',(1)} e^{-iy_t}\right)\right|}{\sum_{x''=1}^{M} q_{x,x'',(1)} \left|\exp\left(\tilde{\lambda}_{x,x'',(1)} e^{-iy_t}\right)\right|} = \frac{q_{\sigma(x),\sigma(x'),(2)} \left|\exp\left(\tilde{\lambda}_{\sigma(x),\sigma(x'),(2)} e^{-iy_t}\right)\right|}{\sum_{x''=1}^{M} q_{\sigma(x),x'',(2)} \left|\exp\left(\tilde{\lambda}_{\sigma(x),x'',(2)} e^{-iy_t}\right)\right|}. \tag{11}$$

Let $x \in \{1,...,M\}$ be fixed. Applying (11) a first time with $x' = x$ and a second time with any x', we get

$$\forall x',\quad \text{for Leb}-a.e.\ y_t,\quad \frac{q_{x,x',(1)} \left|\exp\left(\tilde{\lambda}_{x,x',(1)} e^{-iy_t}\right)\right|}{q_{x,x,(1)} \left|\exp\left(\tilde{\lambda}_{x,x,(1)} e^{-iy_t}\right)\right|} = \frac{q_{\sigma(x),\sigma(x'),(2)} \left|\exp\left(\tilde{\lambda}_{\sigma(x),\sigma(x'),(2)} e^{-iy_t}\right)\right|}{q_{\sigma(x),\sigma(x),(2)} \left|\exp\left(\tilde{\lambda}_{\sigma(x),\sigma(x),(2)} e^{-iy_t}\right)\right|}$$

and so

$$\forall x',\quad \frac{q_{x,x',(1)}}{q_{x,x,(1)}} = \frac{q_{\sigma(x),\sigma(x'),(2)}}{q_{\sigma(x),\sigma(x),(2)}} \tag{12}$$

and

$$\forall x',\quad \tilde{\lambda}_{x,x',(1)} - \tilde{\lambda}_{x,x,(1)} = \tilde{\lambda}_{\sigma(x),\sigma(x'),(2)} - \tilde{\lambda}_{\sigma(x),\sigma(x),(2)}. \tag{13}$$

Now, since $\sum_{x'} q_{x,x',(1)} = 1 = \sum_{x'} q_{\sigma(x),\sigma(x'),(2)}$, due to (12), it comes $q_{x,x,(1)} = q_{\sigma(x),\sigma(x),(2)}$ and so

$$\forall x' \in E,\quad q_{x,x',(1)} = q_{\sigma(x),\sigma(x'),(2)}.$$

Since θ_1 and θ_2 are in Θ', $\sum_{x'} \tilde{\lambda}_{x,x',(1)} = 0 = \sum_{x'} \tilde{\lambda}_{\sigma(x),\sigma(x'),(2)}$, and due to (13), we get $\tilde{\lambda}_{x,x,(1)} = \tilde{\lambda}_{\sigma(x),\sigma(x),(2)}$ and, applying again (13), we conclude that

$$\forall x' \in E,\quad \tilde{\lambda}_{x,x',(1)} = \tilde{\lambda}_{\sigma(x),\sigma(x'),(2)}.$$

□

4 Numerical results and model comparison

4.1 Model selection

Before analyzing any numerical results, one has to discuss the choice of the number of regimes and of the order of the AR models. In practice we found that the BIC criterion generally permits to identify parsimonious models which fit well the data. It is defined as

$$BIC = -2\log L + k\log(N)$$

and L is the likelihood of the data, k is the number of parameters and N is the number of observations. In order to make the final selection among the best models identified by BIC, we have compared their abilities to generate realistic wind time series since this is the main motivation for this work. For this, a large number of realizations of the various models under competition have been simulated and various statistics of these synthetic sequences have been compared with the ones of the original data.

The models were fitted with a number of regimes M varying from 1 to 6 at the most and the BIC values suggest selecting models with $M = 3$ or $M = 4$ regimes (see Tables 1 and 2). For the wind direction the model with $M = 4$ regimes tends to better reproduce the marginal distribution of the process compared to the models with $M = 3$ regimes and we thus have chosen to select this model. The **NHMS-EVM** model with $M = 4$ and $s = 2$, which is used in the **NHMS-AR**$_{(U,\Phi)}$ model, has 43 parameters. For the Cartesian coordinates $\{u_t, v_t\}$ and for the wind intensity $\{U_t\}$ the models with $M = 3$ and $M = 4$ regimes lead to similar results and we have thus chosen to keep the simplest model with $M = 3$.

We also varied the order s of the autoregressive models from $s = 0$ (y_t is independent of y_0^{t-1} given x_t) to $s = 5$ and the BIC values are generally decreasing with s suggesting that a model of order $s \geq 5$ may be needed. Notice however that there is generally a big improvement in the BIC values when s increases from 0 to 1 and from 1 to 2 whereas the difference is much smaller when comparing the models of order $s = 2$ and $s \geq 3$ (not shown). We will focus on models of order $s = 2$ in the sequel. We believe that models of reduced order are more realistic from a physical point of view and we get similar simulation results with $s = 2$ compared to the models with $s \geq 3$.

The BIC of $\{u_t, v_t\}$ models are generally smaller than the ones of $\{U_t, \Phi_t\}$ models except for $s = 0$. It may be due to the higher number of parameters involved in the **NHMS-AR**$_{(U,\Phi)}$ model (66 parameters when $M = 3$), which has two layers of hidden variables whereas the **NHMS-AR**$_{(u,v)}$ model has one common weather type for $\{u_t\}$ and $\{v_t\}$ and only 44 parameters when $M = 3$. Note however that BIC does not permit to make a clear distinction between both parameterizations (polar or Cartesian) since the differences in BIC values are relatively small.

	M	1	2	3	4	5	6	k
Model	s	BIC						
HMS-EVM	1	7778	6326	6334	6307	6277	6385	M(M-1)+4M
NHMS-EVM	1	7778	6266	6171	6141	6158	6372	M(M+1)-1+4M
HMS-EVM	2	7568	5952	5979	5963	6051	6075	M(M-1)+6M
NHMS-EVM	2	7568	5882	5872	**5882**	5968	6075	M(M+1)-1+6M

Table 1: BIC values for the various fitted wind direction models. The last column gives the number of parameters. The bold value corresponds to the selected model.

	M	1	2	3	4	5	k
Model	s			BIC			
HMS-AR$_{(u,v)}$	0	48583	44616	42338	40903	40025	(M(M-1)+5M
NHMS-AR$_{(u,v)}$	0	-	43679	41212	39878	38981	M(M+1)-1+5M
NHMS-AR$_{(U,\Phi)}$	0	-	32553	31180	30381	30000	43+M(M+1)-1+2M
HMS-AR$_{(u,v)}$	1	31979	28134	27561	27219	27079	(M(M-1)+9M
NHMS-AR$_{(u,v)}$	1	-	27687	27110	26855	26755	M(M+1)-1+9M
NHMS-AR$_{(U,\Phi)}$	1	-	28833	28543	28446	28380	43+M(M+1)-1+3M
HMS-AR$_{(u,v)}$	2	30619	26753	**26162**	25950	25947	(M(M-1)+11M
NHMS-AR$_{(u,v)}$	2	-	26275	25681	**25598**	25607	M(M+1)-1+11M
NHMS-AR$_{(U,\Phi)}$	2	-	28458	28266	**28163**	28196	43+M(M+1)-1+4M

Table 2: BIC values for the various bivariate models. The last column gives the number of parameters. The bold values correspond to the selected models.

4.2 Regimes can be interpreted as weather types

An important benefit of using weather type models for meteorological variables is that they generally lead to interpretable models. This is illustrated in this section on **NHMS-AR**$_{(u,v)}$ and **NHMS-AR**$_{(U,\Phi)}$ models. In order to compare the regimes of these two models, they have been ordered according to the variance of the innovation of the autoregressive processes $\Sigma^{(s)}$. Figure 3 shows that the distributions of the wind direction in the different regimes are broadly similar for both models. The first regime corresponds mainly to anticyclonic conditions with easterly wind and a slow varying intensity (the variance of the innovation of the AR model is lower than in the other regimes and the first AR coefficient is larger). This regime is also the most likely (probability of occurrence of about 46%). The two other regimes correspond to cyclonic conditions with westerly wind and higher temporal variability in the intensity. These two regimes are discriminated mainly by the temporal variability, which is higher in the third regime, and the wind direction with the second regime corresponding mainly to south-westerlies and the third regime corresponding mainly to north-westerlies (see Figure 3).

Both **NHMS-AR**$_{(u,v)}$ than in **NHMS-AR**$_{(U,\Phi)}$ models have similar transition probabilities (see Figure 4) with a more pronounced dependence on the wind direction for the **NHMS-AR**$_{(U,\Phi)}$ model. The more persistent regime is clearly the first one (mean duration of about 3.4 days) with a high probability of staying in this regime in any wind direction. The probability of switching directly from regime 1 to regime 3 is very small and the Markov chain will generally transit through the regime 2. Transitions from regime 1 to regime 2 are more likely when the wind is blowing from the west and transitions from regime 2 to regime 3 generally occur when the wind is from south. Regime 3 is persistent only when the wind is from south-west. If the wind blows from other directions, the weather type will quickly switch to regime 1 or 2.

4.3 Marginal distributions

According to Figure 5, the models with non-homogeneous transition probabilities provide a better description of the marginal distribution of the wind direction than homogeneous models which have difficulties in reproducing the second mode of the distribution (associated to easterlies). The **NHMS-AR**$_{(U,\Phi)}$ model seems to perform slightly better than the **NHMS-AR**$_{(u,v)}$ model.

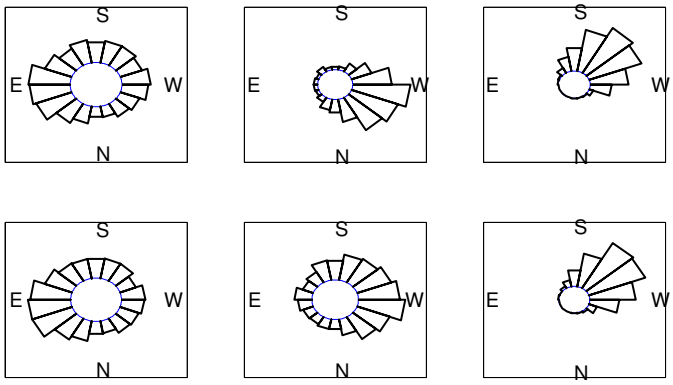

Figure 3: Rose plot of the wind direction in the three regimes identified on wind speed by **NHMS-AR**$_{(U,\Phi)}$ model (top) and by **NHMS-AR**$_{(u,v)}$ model (bottom).

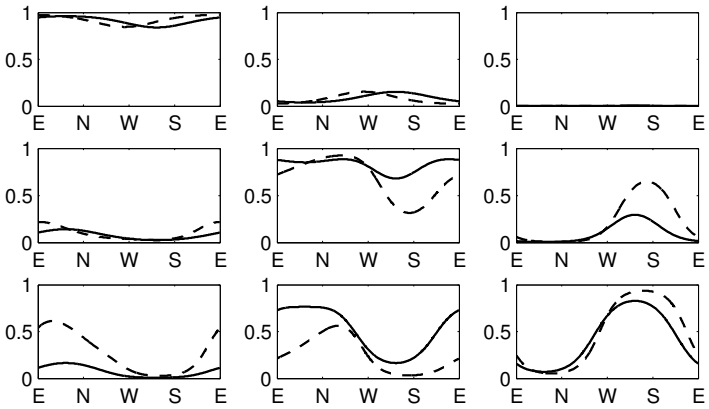

Figure 4: Matrix of non-homogeneous transitions of **NHMS-AR**$_{(u,v)}$ model (plain line) and **NHMS-AR**$_{(U,\Phi)}$ model (dashed line)

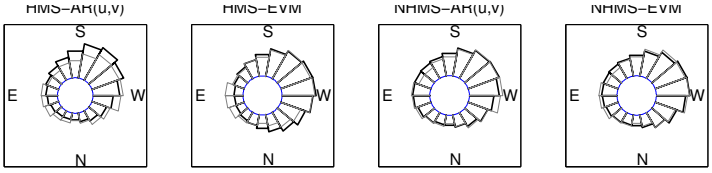

Figure 5: Rose plot of the marginal distribution of wind direction for the various models with $M = 4$ (resp. $M = 3$) regimes for Φ_t (resp.$\{u_t, v_t\}$) and order $s = 2$.

The joint distribution of $\{u_t, v_t\}$ is globally well reproduced by both non-homogeneous models (see Figure 6). Simulated data exhibit two modes like in the original data. The modes seem to be slightly better located with the **NHMS-AR**$_{(U,\Phi)}$ model. It may be due to the small differences in the non-homogeneous transition probabilities shown in Figure 4 with the **NHMS-AR**$_{(U,\Phi)}$ model having a slightly higher probability of staying in regime 3 when the wind is blowing from the south-west. It may help to create two distinct modes at the correct locations.

Both models generate too much low wind and as a consequence fail to reproduce accurately the

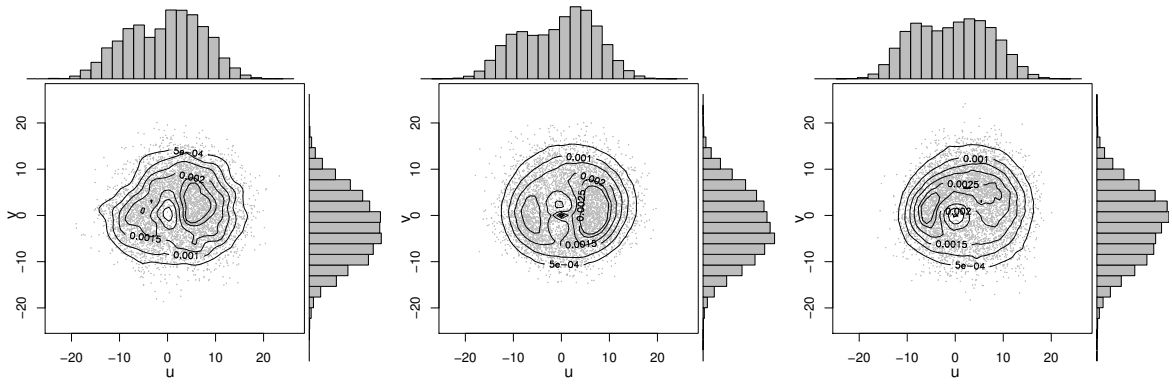

Figure 6: Joint distributions of $\{u_t, v_t\}$ for observed wind (left) and wind simulated with **NHMS-AR**$_{(u,v)}$ model (middle) and **NHMS-AR**$_{(U,\Phi)}$ model (right)

hole at origin. Similar lack of fit for the marginal distribution was observed on other dataset with MS-AR models. It seems to be especially sensible when the model is miss-specified. This discrepancy may be reduced by developing alternative estimation methods which would give more importance to the stationary distribution of the process. This will be the topic of future research.

4.4 Dependence structure

All the models reproduce approximatively the first lags of autocorrelation function of $\{U_t\}$ (see Figure 7) and the circular autocorrelation of Φ (not shown) defined as (see [9])

$$\rho(h) = \frac{E[\cos(Y_0)\cos(Y_h)] + E[\sin(Y_0)\sin(Y_h)] - E[\sin(Y_0)\cos(Y_h)] - E[\cos(Y_0)\sin(Y_h)]}{E[\cos(Y_0)^2]E[\sin(Y_0)^2] - E[\sin(Y_0)\cos(Y_0)]^2} \quad (14)$$

for any positive integer h. To further validate the models, we have also plotted the various terms which appear in (14). According to Figure 8, the autocorrelation function of $\{\cos(\Phi_t)\}$ is generally better reproduced than the one of $\{\sin(\Phi_t)\}$. The empirical autocorrelation of $\{\sin(\Phi_t)\}$ has a more complex shape, with a quick decrease close to the origin and a bump around 4 days, than the one of $\{\cos(\Phi_t)\}$ which exhibits a more monotonic decrease. Figure 7 shows the cross-correlation function between the time series $\{\cos(Y_t)\}$ and $\{\sin(Y_t)\}$. The sample cross-correlation function is at its maximum value for a lag between 18 hours and 24 hours, with the time series $\{\sin(Y_t)\}$ being in advance of the time series $\{\cos(Y_t)\}$. This may be related to the fact that, for the location of interest, the wind direction tends to rotate more often clockwise than anti-clockwise between two successive time steps (see Figure 9). Note that the complex parametrization of the von Mises autoregressive models permits to model rotation in a prevailing direction and significantly improves the boxplot shown on Figure 9 compared to models with real parametrization (not shown). One can also remark that the first order autoregressive matrices of the **NHMS-AR**$_{(u,v)}$ look like rotation matrices with diagonal coefficients which are close to each other and out-diagonal coefficients which are almost opposed. Figure 9 shows however that they do not generate not anticlockwise rotations.

The non-homogeneous models generally lead to a better description of the correlation functions compared to the homogeneous models. All the models lead to an underestimation of the empirical autocorrelations functions of the time series $\{\cos(Y_t)\}$ and $\{\sin(Y_t)\}$ for positive time lags.

Increasing the order s of the autoregressive models leads to a better description of the second order structure of the process but models of order $s \geq 3$ can not reproduce the second mode of the marginal distribution and thus models of order $s = 2$ seem to provide a good compromise.

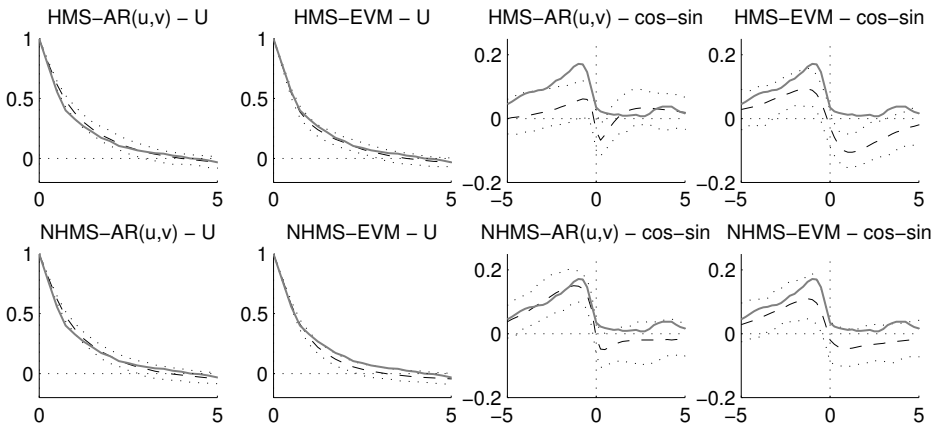

Figure 7: Correlation function of U_t and cross-correlation functions between the time series $\{\cos(Y_t)\}$ and $\{\sin(Y_t)\}$ for the various models. The full grey line corresponds to the sample functions and the dashed line to the fitted model with a 95% prediction intervals (dotted line). The distributions for the fitted model was obtained by simulation. Time on the x-axis is expressed in days.

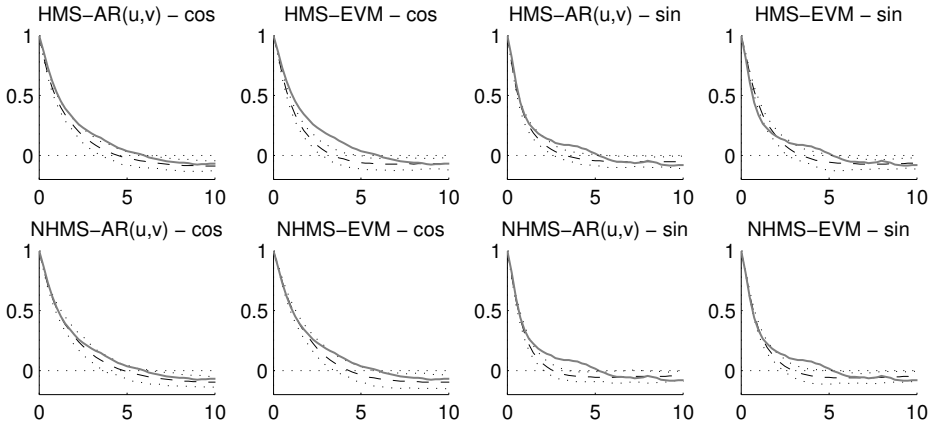

Figure 8: Autocorrelation functions of the time series $\{\cos(Y_t)\}$ and $\{\sin(Y_t)\}$ for the various models. The full grey line corresponds to the sample functions and the dashed line to the fitted model with a 95% prediction intervals (dotted line). The distributions for the fitted model was obtained by simulation. Time on the x-axis is expressed in days.

5 Conclusion

In this paper we propose to model bivariate wind time series considering Cartesian coordinates on one hand and polar coordinates on the other hand. Both approaches have advantages. The $\{u_t, v_t\}$ models is easier to write and to fit since they are based on Gaussian distributions unlike the (U_t, Φ_t) for which one has to use von Mises distributions. The $\{u_t, v_t\}$ model permits to globally well restore the second order structure observed on the data while the $\{U_t, \Phi_t\}$ model

seems to give a better description of the marginal distributions. However, the differences between both models are slight.

All the models are based on MS-AR modeling and versions with homogeneous and non-homogeneous probability transition functions are compared. In non-homogeneous models, the transitions depend on the wind direction at the previous time. At the location of interest, wind is rotating more often clockwise but wind direction may also oscillate around two prevailing directions (northeast for anti-cyclonic conditions and southwest for cyclonic conditions). These features induce respectively some cycles which can be seen in the second order structure and modes in the marginal distribution. In broad outline, non-homogeneous transitions help the process to stay in the same weather regime when the wind direction is close to the main directions. In order to generate the cycles, it is necessary to command the wind direction to turn in the right direction. In $\{u_t, v_t\}$ models the rotations are reproduced by the autoregressive A matrices, but they are specified more naturally in **NHMS-EVM** model by using a complex parametrization of the von Mises autoregressive models.

At last, the proposed models allow to generate wind time series with features very close to the main features of the observed time series. The introduction of the latent state allow to simulate the different time scale which are present in the data, with the autoregressive part describing the short-term fluctuations whereas the weather type, which lasts typically a few days, describes longer-term fluctuations. An other layer could be added to simulate shorter time scales for very local features. The model could also be extended to a space-time model in several ways. For this, it will probably be easier to work with the $\{u_t, v_t\}$ model based on Gaussian distributions which can naturally handle a space-time information. Then several strategies could be considered for the weather type process which could be local, with a different weather type at each site, or regional with a common weather type for the different locations. With the first strategy one has to deal with a space-time process of latent discrete variables and this is challenging from both a modeling and computational point of view. The second strategy is probably simpler to implement but requires some space-time homogeneity in the data. These and other related modeling issues remain to be investigated.

References

[1] P. Ailliot and Pène F. Consistency of the maximum likelihood estimate for non-homogeneous markov-switching models.

[2] P. Ailliot and V. Monbet. Markov-switching autoregressive models for wind time series. *Environmental Modelling and Software*, 30:92–101, 2012.

[3] P. Ailliot, V. Monbet, and M. Prevosto. An autoregressive model with time-varying coefficients for wind fields. *Environmetrics*, 17(2):107–117, 2006.

[4] P. Ailliot, C. Thompson, and P. Thomson. Space time modeling of precipitation using a hidden markov model and censored gaussian distributions. *Journal of the Royal Statistical Society, Series C (Applied Statistics)*, 58(3):405–426, 2009.

[5] L.E. Baum, T. Petrie, G. Soules, and N. Weiss. A Maximization Technique Occurring in the Statistical Analysis of Probabilistic Functions of Markov chains. *The Annals of Mathematical Statistics*, 41(1):164–171, 1970.

[6] J. Breckling. *The Analysis of Directional Time Series: Applications to Wind Speed and Direction*, volume 61 of *Lecture Notes in Statistics*. Springer, Berlin, Germany, 1989.

[7] O. Cappé, E. Moulines, and Rydén T. *Inference in hidden Markov models*. Springer-Verlag, New York, 2005.

[8] A. P. Dempster, Laird N. M., and D. B. Rubin. Maximum likelihood from incomplete data via the em algorithm. *Journal of the Royal Statistical Society: Series B (Statistical Methodology)*, 39(1):1–38, 1977.

[9] N.I. Fisher and A. J. Lee. A correlation coefficient for circular data. *Biometrika*, 70:327–332, 1983.

[10] N.I. Fisher and J. Lee. Time series analysis of circular data. *Journal of the Royal Statistical Society: Series B (Statistical Methodology)*, 56:327–339, 1994.

[11] M.D. Fraser, Y.S. Hsu, and Walker J.J. Identifiability of finite mixtures of von mises distributions. *Annals of statistics*, 9:1130–1131, 1981.

[12] Montserrat Fuentes, Li Chen, Jerry M Davis, and Gary M Lackmann. Modeling and predicting complex space–time structures and patterns of coastal wind fields. *Environmetrics*, 16(5):449–464, 2005.

[13] H Hajo Holzmann, A. Munk, M. Suster, and W. Zucchini. Hidden markov models for circular and linear-circular time series. *Environmental and Ecological Statistics*, 13:325–347, 2006.

[14] J.D. Hamilton. Analysis of time series subject to changes in regime. *Journal of Econometrics*, 45:39–70, 1990.

[15] A. S. Hering and M. G. Genton. Powering up with space-time wind forecasting. *Journal of the American Statistical Association*, 105(489):92–104, 2010.

[16] Matthias Hofmann and Iver Bakken Sperstad. Nowicob–a tool for reducing the maintenance costs of offshore wind farms. *Energy Procedia*, 35:177–186, 2013.

[17] J. P. Hughes, Guttorp P., and S. P. Charles. A non-homogeneous hidden markov model for precipitation occurrence. *Applied Statistics*, pages 15–30, 1999.

[18] S. Kato. A markov process for circular data. *Journal of the Royal Statistical Society: Series B (Statistical Methodology)*, 72:655–672, 2010.

[19] K.V Mardia. *Statistics of directional data*. Academic press, New York, 1972.

[20] H. Tong. *Non-Linear Time Series: A Dynamical System Approach*. Oxford University Press, Oxford, U.K., 1990.

[21] Christopher K Wikle, Ralph F Milliff, Doug Nychka, and L Mark Berliner. Spatiotemporal hierarchical bayesian modeling tropical ocean surface winds. *Journal of the American Statistical Association*, 96(454):382–397, 2001.

[22] W. Zucchini and P. Guttorp. A hidden Markov model for space-time precipitation. *Water Resources Research*, 27:1917–1923, 1991.

[23] W. Zucchini and I. MacDonald. *Hidden Markov Models for Time Series: An Introduction Using R.* Number 110 in Monographs on statistics and applied probability. CRC Press, 2009.

Figure 9: Frequency of anticlockwise rotations between successive observations for the various models with $M = 4$ regimes and autoregressive model of order $s = 2$. The grey line corresponds to the value obtained on the data (45.4 % of anticlockwise rotations against 54.6 % of clockwise rotations). The boxplots show the distributions for the fitted models. They were obtained by simulation (results based on 4400 time series of length 124). Le xlabel est coupe